BJR

https://doi.org/10.1259/bjr.20201204

Received: 06 October 2020 | Revised: 07 March 2021 | Accepted: 10 March 2021

Cite this article as:
Krishnaraju VS, Singh H, Kumar R, Sharma S, Mittal BR, Bhattacharya A. Infection imaging using [18F]FDG-labelled white blood cell positron emission tomography–computed tomography. *Br J Radiol* 2021; **94**: 20201204.

PICTORIAL REVIEW

Infection imaging using [18F]FDG-labelled white blood cell positron emission tomography–computed tomography

VENKATA SUBRAMANIAN KRISHNARAJU, MD, HARMANDEEP SINGH, MD, RAJENDER KUMAR, MD, SARIKA SHARMA, PhD, BHAGWANT RAI MITTAL, MD, DNB and ANISH BHATTACHARYA, DNB, PhD

Department of Nuclear Medicine, Post Graduate Institute of Medical Education and Research, Chandigarh, India

Address correspondence to: Dr Anish Bhattacharya
E-mail: *anishpgi@yahoo.co.in*

ABSTRACT

Localizing the sites of infection in the body is possible in nuclear medicine using a variety of radiopharmaceuticals that target different components of the infective and inflammatory cascade. Gamma(γ)-emitting agents such as [67Ga]gallium citrate were among the first tracers used, followed by development of positron-emitting tracers like 2-deoxy-2-[18F]fluoro-D-glucose (^{18}F-FDG). Though these tracers are quite sensitive, they have limited specificity for infection due to their concentration in sites of non-infective inflammation. White blood cells (WBC) labelled with γ or positron emitters have higher accuracy for differentiating the infective processes from the non-infective conditions that may show positivity with tracers such as ^{18}F-FDG. We present a pictorial review of potential clinical applications of PET/CT using ^{18}F-FDG labelled WBC.

INTRODUCTION

Infection is a pathological process that can present with a wide range of manifestations based on the site, extent, severity and the pathogen that is inciting the disease process. Clinical symptoms and signs may help in localizing the site of infection with the help of laboratory parameters such as leukocyte count, erythrocyte sedimentation rate and C-reactive protein which serve as markers for infection and associated inflammation. Anatomical imaging techniques including X-ray, CT and MRI are useful in infection imaging, based on the site of disease. However, these imaging methods are not sensitive for the detection of infective processes at early stages before anatomical changes set in.[1]

Nuclear medicine functional imaging techniques can help in overcoming these shortcomings. Infection imaging in nuclear medicine involves use of both γ and positron-emitting radiopharmaceuticals. [67Ga]gallium citrate and 2-deoxy-2-[18F]fluoro-D-glucose (^{18}F-FDG) are sensitive for infection but are non-specific, as they may accumulate in sites of sterile non-infective inflammation which is frequently seen in patients who have undergone a surgical procedure or following insertion of a prosthetic device.[2] This limitation can be overcome by more specific agents that target specific processes such as radiolabelled antibiotics (such as ciprofloxacin and fluconazole), radiolabelled monoclonal antibodies targeted against specific receptors on the surface of leukocytes, radiolabelled cytokines or chemokines and labelled white blood cells (WBC).[1,3]

Radiotracers available for WBC labelling include gamma-emitting agents such as [111In]In-oxine[4] and [99mTc]Tc-HMPAO,[5] and positron-emitting agents such as ^{18}F-FDG. Basic equipment and time required for the WBC labelling procedure is similar for different radiotracers. However, the cost of the radiotracer will vary from one region to another. Institutions equipped with a medical cyclotron may prefer to use ^{18}F-FDG produced in-house, rather than purchase [111In]In-oxine or HMPAO kits.[6–9] Despite the higher specificity of radiolabelled WBC, the main disadvantage of gamma-emitting agents such as indium-111 was their poor imaging characteristics.[2] The protocol for a labelled WBC study using gamma-emitting agents involves an early image at 0.5–1 h, a delayed scan at 3–4 h and a late image at 20–24 h.[4,5] This allows for sufficient background tracer activity clearance from the blood pool and better visualization of lesions. Delayed imaging with ^{18}F-FDG-labelled WBC is not possible due to the shorter half-life of ^{18}F. However, the superior imaging

Figure 1. MIP image of ^{18}F-FDG-labelled WBC whole body PET/CT in a patient with aortic graft infection following antibiotic therapy. The image shows physiological distribution in the spleen, liver and the bone marrow.[11] The labelling efficiency of the radiopharmaceutical in this case was 90.3%. No area of abnormal tracer uptake is seen. However, mild brain uptake due to minimal free ^{18}F-FDG activity and excretion via the kidneys into the urinary bladder is also noticed. FDG, fluoro-D-glucose; MIP, maximum intensity projection; PET, positron emission tomography; SUV, standardized uptake value; WBC, white blood cell.

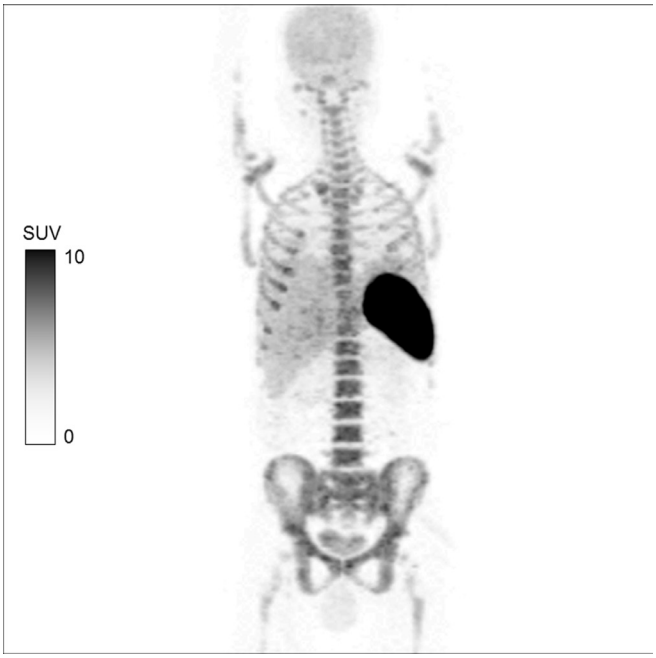

characteristics of ^{18}F-FDG ensure that the diagnostic performance of ^{18}F-FDG-labelled WBC is comparable to [111In] In-oxine labelled WBC.[7] In infective foci with low neutrophil response, the lack of delayed images may result in false-negative results and studies with WBC labelled with longer lived positron emitters may be required to clarify this issue.

^{18}F-FDG-labelled WBC labelling procedure

Bhattacharya et al[8] modified the *in-vitro* method of radiolabelling of WBC to allow for labelling with ^{18}F-FDG under sterile aseptic conditions. While all WBC labelling methods follow the same basic principle, there are significant differences in the successive steps for labelling WBCs using [99mTc], [111In] or ^{18}F-FDG. The final labelling efficiency varies widely depending on which of these tracers / methods is used. As reported by Meyer et al[10], the study by Bhattacharya et al[8] used the lowest amount of ^{18}F-FDG with the highest labelling efficiency. In this method, about 40 ml of the patient's blood is drawn into a heparinized syringe. The red blood cells are removed by sedimentation and the WBC rich plasma is then centrifuged to separate the pellet containing WBCs. This WBC pellet is reconstituted in heparinized normal saline and incubated at 37°C with ^{18}F-FDG for labelling the WBCs. The labelled cells are reconstituted with cell-free plasma obtained during centrifugation and the reconstituted preparation injected into the patient. The labelling efficiency by this method was found to be 81 ± 17%.[8] Though the labelling efficiency with ^{18}F-FDG was lower in other studies, the diagnostic performance was comparable to other γ-emitting agents.[10] Radiochemical purity has to be ensured before injection as the presence of higher quantities of free ^{18}F-FDG may lead to physiological uptake in organs such as the brain (Figure 1) and to a decrease in specificity due to free ^{18}F-FDG uptake by non-infective inflammatory processes.

About 148–185 MBq of ^{18}F-FDG-labelled WBCs are injected into the patient and optimal imaging time is 120 min post-injection. The field of imaging can be whole body or limited to the region of interest only. The normal biodistribution of ^{18}F-FDG-labelled WBCs is shown in the positron emission tomography (PET) image in Figure 1. In a meta-analysis done by Meyer et al, [18F] FDG-labelled WBC PET/CT was found to have a higher diagnostic accuracy than conventional modalities such as CT or MRI and ^{18}F-FDG PET/CT. An area of focal increased tracer uptake is interpreted as positive for infection on ^{18}F-FDG-labelled WBC PET/CT. However, no definite cut-off of standardized uptake value (SUV) was identified to reliably suggest presence of infection in this meta-analysis of five studies evaluating SUV parameters in labelled ^{18}F-FDG-labelled WBC PET/CT.[10]

Potential clinical indications

Due to its high sensitivity, ^{18}F-FDG PET/CT is the first-line diagnostic imaging modality for evaluating patients with fever of unknown origin as this symptom can be caused by infection or malignancy.[12] However, radiolabelled WBC imaging has been reported to be useful in localizing the site and extent of infections in a wide range of conditions with a higher specificity. The clinical indications investigated with ^{18}F-FDG-labelled WBC to date include infections in renal cysts, in peripancreatic fluid collections in cases of pancreatitis, as well as diagnosing prosthesis-related infections and exclusion of diagnosis of osteomyelitis.[10]

Figure 2 shows the use of ^{18}F-FDG-labelled WBC PET/CT contributing to the diagnosis of skull base osteomyelitis in a diabetic patient with recurrent middle ear infection in a post-surgical patient. The advantage of ^{18}F-FDG-labelled WBC PET/CT in this condition is the ability to delineate active infection from post-surgical inflammatory changes. The lack of normal physiological uptake of ^{18}F-FDG-labelled WBC in the brain parenchyma as compared to ^{18}F-FDG enhances visual assessment of tracer uptake at the site of skull base infection.

Figures 3–5 show the potential utility of ^{18}F-FDG-labelled WBC PET/CT in patients with infections of cardiac implants and following cardiovascular surgical procedures. ^{18}F-FDG-labelled WBC PET/CT can diagnose the presence of infection and can also localize the site and extent of the infection, thereby, directing the patient towards appropriate management procedures.[13] ^{18}F-FDG-labelled WBC PET/CT can also predict whether a collection seen in the abdominal cavity is infected or sterile based on the results that have been seen in patients with peripancreatic fluid collection.[8] Figure 6 shows one such patient with infected peripancreatic collection. ^{18}F-FDG-labelled WBC PET/CT may also have a potential role in assessing the extent

Figure 2. A 64-year-old diabetic male with left-sided chronic suppurative otitis media, underwent left-sided MRM and tympanoplasty. 8 months later, he developed recurrent discharge in the left ear with new onset pain and discharge in the right ear. Axial CT image (a) shows post-operative changes of MRM in the left ear. The MIP ^{18}F-FDG-labelled WBC PET/CT (b), axial CT (c, e) and fused PET/CT (d, f) images showed radiolabelled WBC accumulation in the left middle ear and along the eustachian tube region (b & d: white arrows, SUVmax 23.2). Radiolabelled WBC accumulation was also noted in subtle sclerotic changes in the sphenoid bone and right skull base suggestive of skull base osteomyelitis (b & f: black arrows, SUVmax 27.4). FDG, fluoro-D-glucose; MRM, modified radical mastoidectomy; PET, positron emission tomography; SUV, standardized uptake value; WBC, white blood cell.

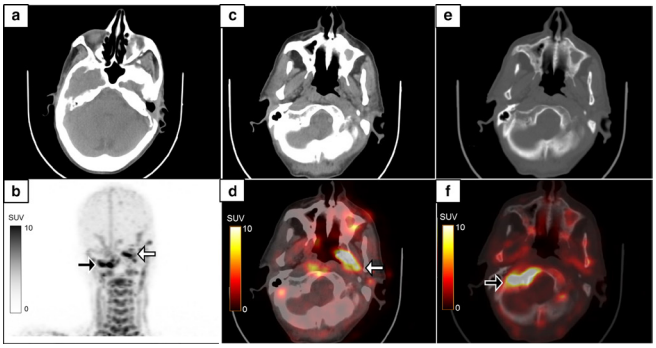

Figure 3. A 23-year-old male who underwent Bentall procedure for aortic aneurysm, presented with recurrent fever and tachycardia. He had graft replacement of the aortic valve, aortic root and the proximal ascending aorta as a part of the procedure. Blood culture was suggestive of infection with *Acinetobacter baumannii*. The MIP ^{18}F-FDG-labelled WBC PET/CT (a) shows an abnormal focus of tracer uptake in the mediastinum (white arrow). The axial PET (b), CECT (c) and fused PET/CT (d) images localized the activity to radiolabelled WBC accumulation (d: white arrow, SUVmax 5.6) in a minimal fluid collection and thickening surrounding the aortic root graft which was seen to extend along the proximal ascending aorta on the sagittal CT (e) and fused PET/CT images (f, white arrow). In view of the difficulty in accessing the site of collection for confirmation of infection, intravenous antibiotics were started based on the blood culture reports and signs of infection subsequently resolved. CECT, contrast-enhanced CT; FDG, fluoro-D-glucose; MIP, maximum intensity projection; PET, positron emission tomography; SUV, standardized uptake value; WBC, white blood cell.

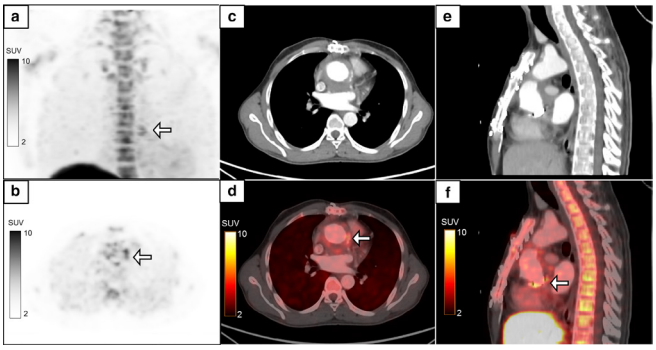

Figure 4. A 72-year-old male with dilated cardiomyopathy had a past history of pacemaker implantation in the left chest wall. He then developed pus discharge from the pacemaker site, and hence the pacemaker was removed and reimplanted on the right side. He still had pus discharge from the left chest wall with a negative pus culture. MIP image (a) of the regional ^{18}F-FDG-labelled WBC PET/CT performed with a suspicion of persistent infection showed a focus of tracer uptake in the left chest wall (B, white arrow, SUVmax 8.9) which localized to the pacemaker leads in the left chest wall on the axial (c, d) and coronal (e, f) CT and fused PET/CT images. A repeat pus culture from the tracer-avid site revealed infection with *Citrobacter sedlakii*. Subsequently the pacemaker leads were removed and the patient became asymptomatic. FDG, fluoro-D-glucose; MIP, maximum intensity projection; PET, positron emission tomography; SUV, standardized uptake value; WBC, white blood cell.

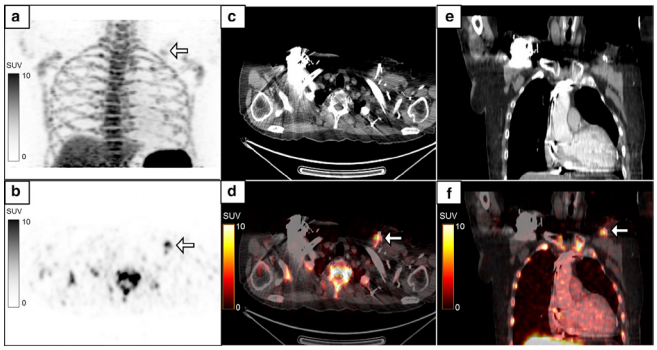

Figure 5. A 74-year-old male, a case of aortoiliac occlusive disease, underwent aorto-bifemoral bypass and prosthetic grafting 1year back. He presented with complaints of pus discharge from the wound in the right groin, which was positive for infection with *Proteus mirabilis*. MIP image (a) of the ^{18}F-FDG-labelled WBC PET/CT done to assess extent of infection showed linear tracer activity in the right iliac region which on the coronal images (b–d, white arrows, SUVmax 5.2) localized to the collection along the bypass graft in the right hemipelvis extending to the right groin (e, f, white arrow). The patient recovered following debridement and drainage of the pus along with a course of intravenous antibiotics. FDG, fluoro-D-glucose; MIP, maximum intensity projection; PET, positron emission tomography; SUV, standardized uptake value; WBC, white blood cell.

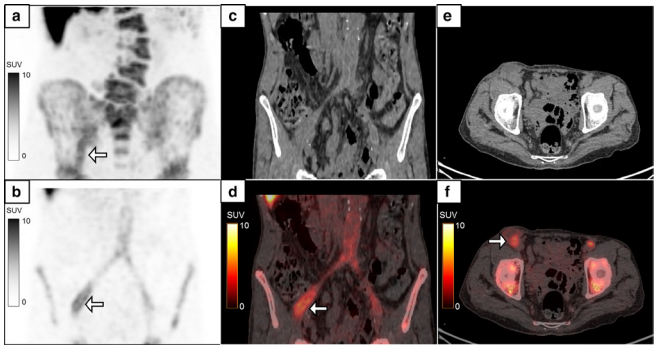

Figure 6. A 40-year-old male presented with complaints of acute onset abdominal pain and vomiting. CECT abdomen was suggestive of necrotizing pancreatitis with peripancreatic collection. MIP image of the ^{18}F-FDG-labelled WBC PET/CT (a) showed heterogeneous tracer activity in the abdominal cavity (white arrow) with another area of diffusely increased homogeneous tracer activity in the left hemithorax (black arrow). The radiolabelled WBC accumulation was localized to the walls of the peripancreatic collections (b, c, white arrow, SUVmax 19.3) and in the consolidation/collapse of left lung lower lobe with left moderate pleural effusion (d, e, black arrow). Necrosectomy of the pancreas showed presence of bacterial colonies in the necrotic tissue. CECT, contrast-enhanced CT; FDG, fluoro-D-glucose; MIP, maximum intensity projection; PET, positron emission tomography; SUV, standardized uptake value; WBC, white blood cell.

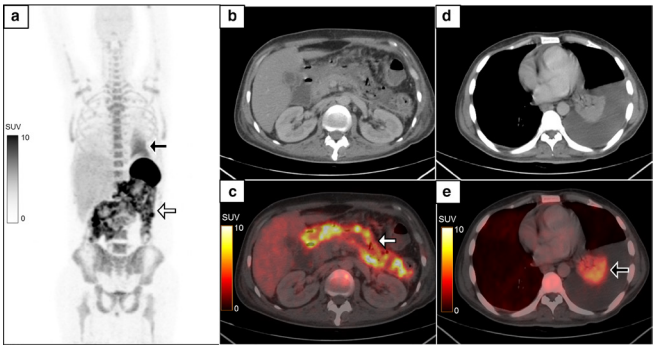

and severity of colitis (Figure 7). The advantage over ^{18}F-FDG PET/CT is the complete absence of any normal physiological bowel uptake that is often seen with ^{18}F-FDG.

Figures 8 and 9 show the potential role of ^{18}F-FDG-labelled WBC PET/CT in assessing infection in patients with orthopedic infections – both following the removal of implants and with implants *in-situ*. The advantage of ^{18}F-FDG-labelled WBC PET/CT in this condition lies in the fact that a conventional three-phase radionuclide bone scan or ^{18}F-FDG PET/CT may show significant false-positive activity in bones with residual reactive changes following orthopedic surgery.[14] This role can also be potentially extended to patients with diabetic cellulitis (Figure 10) where ^{18}F-FDG-labelled WBC PET/CT can help in ruling out presence of any infective bone involvement.[15] Though the ^{18}F-FDG-labelled WBC study is only used in a research setting in some centers, it is performed as a part of routine clinical management in our institute. However, all the patients undergoing the procedure, including those mentioned in this review, signed an informed consent before undergoing the procedure.

Potential false-positives and false-negatives

Imaging using ^{18}F-FDG-labelled WBC PET/CT is based on the principle of enhanced vascular permeability and chemokine-induced rapid neutrophil aggregation at sites of acute inflammation which leads to accumulation of radiolabelled WBCs. It does not involve direct imaging of the pathogenic organisms, and so false-positive results can be seen in sites of acute non-infectious inflammation with neutrophil accumulation such as inflammatory bowel disease (Figure 11). Other causes of a false-positive

Figure 7. A 25-year-old male presented with complaints of long-standing abdominal pain and diarrhea. He was suspected to have inflammatory bowel disease on initial clinical and radiological evaluation. MIP image (a) of ^{18}F-FDG-labelled WBC PET/CT showed increased tracer uptake in a long bowel segment involving the descending and sigmoid colon (white arrow) and the rectum with a few foci of tracer activity in the right iliac fossa (black arrow). Coronal CECT (b) and fused PET/CT images (c) localized the radiolabelled WBC accumulation to a circumferential mural thickening involving the distal colon and rectum (white arrows, SUVmax 14.2) which was also seen on the axial CECT (d) and fused PET/CT images (e) along with another focus of tracer avidity in the thickened terminal ileum (black arrow, SUVmax 15.5). Colonoscopy with biopsy confirmed the diagnosis of Crohn's disease with active bacterial colitis. However, ^{18}F-FDG-labelled WBC PET/CT may also show uptake in non-infective inflammatory bowel disease as shown in Figure 11. Lack of physiological tracer uptake in normal bowel loops is an advantage over ^{18}F-FDG PET. CECT, contrast-enhanced CT; FDG, fluoro-D-glucose; MIP, maximum intensity projection; PET, positron emission tomography; SUV, standardized uptake value; WBC, white blood cell.

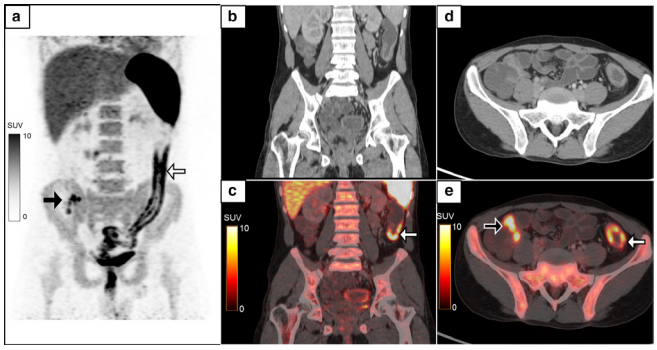

study include apparent increase in tracer activity due to anatomical factors such as blood flow confined to a small volume as in a case of collapsed lung (Figures 6 and 11), poor labelling of the WBC with ^{18}F-FDG resulting in non-specific accumulation of free ^{18}F-FDG and extravasation from hemorrhagic lesions.[10]

The potential false negatives include chronic infection and inflammation which has a predominant lymphocyte and macrophage infiltration, prior exposure to effective antibiotic therapy and in immunosuppressed hosts with poor immune response. Vertebral osteomyelitis is also seen to have a lower grade of radiolabelled WBC accumulation.[10]

Drawbacks of ^{18}F-FDG-labelled WBC PET/CT

Though ^{18}F-FDG-labelled WBC PET/CT has numerous potential indications as discussed, there are some drawbacks as compared to ^{18}F-FDG PET/CT such as requirement of skilled technical expertise for labelling, increase in total duration of the investigation to account for the time required for the labelling procedure, potential costs involved with the required setup for labelling, need to maintain sterility during handling of blood products and the inherent risks associated with injection of blood and blood products.[16] Eventually, the short half-life of ^{18}F does not allow delayed images acquisition beyond 120 min which

Figure 8. A 43-year-old female presented with pain and pus discharge from the right lower leg. She had a past history of compound fracture of the right tibia and fibula 8 years previously, for which she had an external fixator in place, which was subsequently removed after 1 year. MIP image (a) of the regional ^{18}F-FDG-labelled WBC PET/CT showed multiple foci of radiolabelled WBC accumulation (white arrows) in the right leg, which corresponded to the sites of pin insertion. PET-CT images show increased tracer uptake (SUVmax 5.5) and CT changes in the form of sinus tract, sequestrum (b, c) and reactive sclerosis (d, e). The symptoms subsided following a course of antibiotics. FDG, fluoro-D-glucose; MIP, maximum intensity projection; PET, positron emission tomography; SUV, standardized uptake value; WBC, white blood cell.

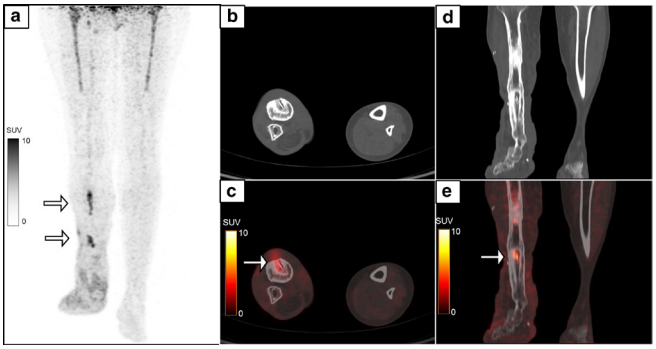

is possible using gamma-emitting agents. *In-vitro* studies using newer agents labelled with long-lived positron emitting agents

Figure 9. A 32-year-old male with fracture of the shaft of the left femur, was treated with PFN. He then developed pus discharge from the left hip 3 weeks following the procedure. MIP image (a) of the ^{18}F-FDG-labelled WBC PET/CT showed a vertical linear focus of radiolabelled WBC accumulation in the left thigh (white arrow) with another horizontal linear focus extending to the skin surface of the left lateral thigh (black arrow). The vertical linear uptake corresponded to the peri-implant region surrounding the PFN on the coronal reformatted images. (b–d, white arrow, SUVmax 5.6) and the horizontal focus localized to the sinus tract on the transaxial images (e, f black arrow, SUVmax 3.4). Exploration and debridement was done and the culture was positive for *Acinetobacter*. FDG, fluoro-D-glucose; MIP, maximum intensity projection; PET, positron emission tomography; PFN, proximal femoral nail; SUV, standardized uptake value; WBC, white blood cell.

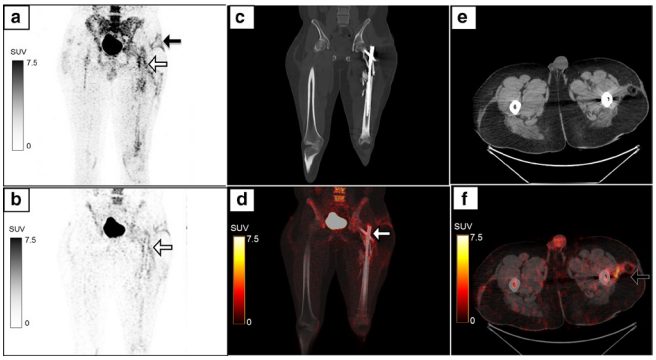

Figure 10. A 67-year-old diabetic female with history of pain, fever and pus discharge from the left leg was diagnosed to have cellulitis. She underwent wound debridement and ^{18}F-FDG-labelled WBC PET/CT to assess the extent of infection and to look for bone involvement. The MIP image (a) showed multiple areas of linear and patchy radiolabelled WBC accumulation in the left leg which was localized to the pus discharging ulcers in the medial and lateral aspects of the leg (b, c white arrow, SUVmax 33.5). There was also linear tracer activity along the collection in the left triceps surae muscles (d, e white arrow) with foci of air within suggesting infection. No evidence of osteomyelitis was noted. The patient responded to a course of intravenous antibiotics with resolution of symptoms. FDG, fluoro-D-glucose; MIP, maximum intensity projection; PET, positron emission tomography; SUV, standardized uptake value; WBC, white blood cell.

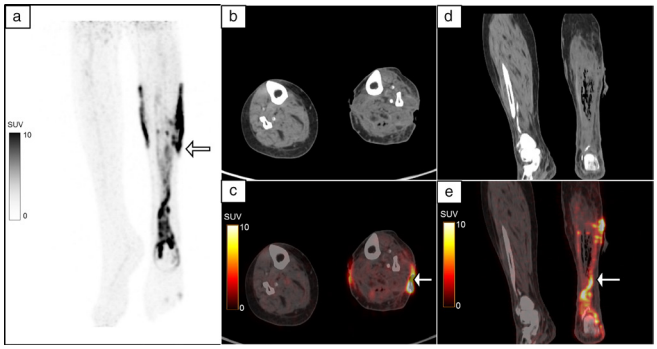

Figure 11. False-positive ^{18}F-FDG-labelled WBC PET/CT is seen in cases of inflammatory bowel disease which is seen in a 27-year-old female with MIP (a, white arrow) showing diffusely increased tracer uptake in the ileal loops and caecum. Transaxial CECT (b) and fused PET/CT (c) shows radiolabelled WBC accumulation (SUVmax 7.8) in the enhancing wall thickening in the distal ileal loops with increased vascularity. Biopsy from the terminal ileum revealed Crohn's disease. Another 42-year-old male with suspected infected peri-pancreatic collection underwent ^{18}F-FDG-labelled WBC PET/CT which showed an abnormal area of tracer activity in the lower zones of the bilateral lung fields (MIP, d, white arrow). Transaxial CT (e) and fused PET/CT (f) localized the radiolabelled WBC accumulation (SUVmax 9.7) to passive collapse in the bilateral lower lobes secondary to pleural effusion. The patient had no symptoms suggestive of any respiratory infection. CECT, contrast-enhanced CT; FDG, fluoro-D-glucose; MIP, maximum intensity projection; PET, positron emission tomography; PFN, proximal femoral nail; SUV, standardized uptake value; WBC, white blood cell.

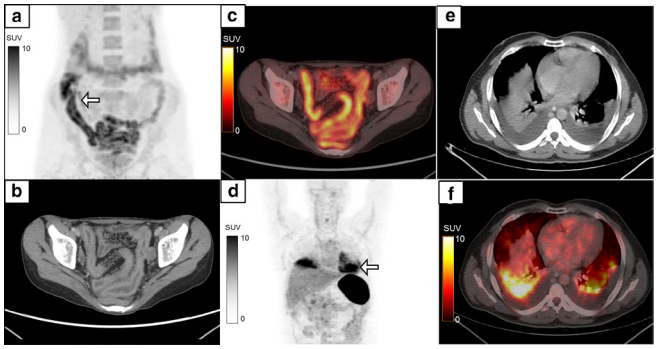

such as copper-64 and zirconium-89 are being investigated to enable delayed imaging.[17,18]

CONCLUSION

^{18}F-FDG-labelled WBC PET/CT might be of interest for diagnosing the presence of infection in suspected cases and for assessing the extent and severity of infection which can help in guiding appropriate management decisions. However, routine clinical use is currently not recommended due to limited data available in the literature and drawbacks associated with the labeling procedure.

REFERENCES

1. Salmanoglu E, Kim S, Thakur ML. Currently available radiopharmaceuticals for imaging infection and the Holy Grail. *Semin Nucl Med* 2018; **48**: 86–99. doi: https://doi.org/10.1053/j.semnuclmed.2017.10.003
2. Vaidyanathan S, Patel CN, Scarsbrook AF, Chowdhury FU. FDG PET/CT in infection and inflammation--current and emerging clinical applications. *Clin Radiol* 2015; **70**: 787–800. doi: https://doi.org/10.1016/j.crad.2015.03.010
3. Goldsmith SJ, Vallabhajosula S. Clinically proven radiopharmaceuticals for infection imaging: mechanisms and applications. *Semin Nucl Med* 2009; **39**: 2–10. doi: https://doi.org/10.1053/j.semnuclmed.2008.08.002
4. Roca M, de Vries EFJ, Jamar F, Israel O, Signore A. Guidelines for the labelling of leucocytes with (111)In-oxine. Inflammation/Infection Taskgroup of the European Association of Nuclear Medicine. *Eur J Nucl Med Mol Imaging* 2010; **37**: 835–41. doi: https://doi.org/10.1007/s00259-010-1393-5
5. de Vries EFJ, Roca M, Jamar F, Israel O, Signore A. Guidelines for the labelling of leucocytes with (99m)Tc-HMPAO. Inflammation/Infection Taskgroup of the European Association of Nuclear Medicine. *Eur J Nucl Med Mol Imaging* 2010; **37**: 842–8. doi: https://doi.org/10.1007/s00259-010-1394-4
6. Osman S, Danpure HJ. The use of 2-[18F] fluoro-2-deoxy-D-glucose as a potential in vitro agent for labelling human granulocytes for clinical studies by positron emission tomography. *Int J Rad Appl Instrum B* 1992; **19**: 183–90. doi: https://doi.org/10.1016/0883-2897(92)90006-K
7. Rini JN, Bhargava KK, Tronco GG, Singer C, Caprioli R, Marwin SE, et al. PET with FDG-labeled leukocytes versus scintigraphy with 111In-oxine-labeled leukocytes for detection of infection. *Radiology* 2006; **238**: 978–87. doi: https://doi.org/10.1148/radiol.2382041993
8. Bhattacharya A, Kochhar R, Sharma S, Ray P, Kalra N, Khandelwal N, et al. PET/CT with 18F-FDG-labeled autologous leukocytes for the diagnosis of infected fluid collections in acute pancreatitis. *J Nucl Med* 2014; **55**: 1267–72. doi: https://doi.org/10.2967/jnumed.114.137232
9. Dumarey N, Egrise D, Blocklet D, Stallenberg B, Remmelink M, del Marmol V, Marmol del V, et al. Imaging infection with 18F-FDG-labeled leukocyte PET/CT: initial experience in 21 patients. *J Nucl Med* 2006; **47**: 625–32.
10. Meyer M, Testart N, Jreige M, Kamani C, Moshebah M, Muoio B, et al. Diagnostic performance of PET or PET/CT using 18F-FDG labeled white blood cells in infectious diseases: a systematic review and a bivariate meta-analysis. *Diagnostics* 2019; **9**: 60. doi: https://doi.org/10.3390/diagnostics9020060
11. Forstrom LA, Dunn WL, Mullan BP, Hung JC, Lowe VJ, Thorson LM. Biodistribution and dosimetry of [(18)F]fluorodeoxyglucose labelled leukocytes in normal human subjects. *Nucl Med Commun* 2002; **23**: 721–5. doi: https://doi.org/10.1097/00006231-200208000-00004
12. Kouijzer IJE, Mulders-Manders CM, Bleeker-Rovers CP, Oyen WJG. Fever of unknown origin: the value of FDG-PET/CT. *Semin Nucl Med* 2018; **48**: 100–7. doi: https://doi.org/10.1053/j.semnuclmed.2017.11.004
13. Yilmaz S, Aliyev A, Ekmekcioglu O, Ozhan M, Uslu L, Vatankulu B, et al. Comparison of FDG and FDG-labeled leukocytes PET/CT in diagnosis of infection. *Nuklearmedizin* 2015; **54**: 262–71. doi: https://doi.org/10.3413/Nukmed-0724-15-02
14. Aksoy SY, Asa S, Ozhan M, Ocak M, Sager MS, Erkan ME, et al. Fdg and FDG-labelled leucocyte PET/CT in the imaging of prosthetic joint infection. *Eur J Nucl Med Mol Imaging* 2014; **41**: 556–64. doi: https://doi.org/10.1007/s00259-013-2597-2
15. Rastogi A, Bhattacharya A, Prakash M, Sharma S, Mittal BR, Khandelwal N, et al. Utility of PET/CT with fluorine-18-fluorodeoxyglucose-labeled autologous leukocytes for diagnosing diabetic foot osteomyelitis in patients with Charcot's neuroarthropathy. *Nucl Med Commun* 2016; **37**: 1253–9. doi: https://doi.org/10.1097/MNM.0000000000000603
16. Dibble EH, Yoo DC, Baird GL, Noto RB. FDG PET/CT of infection: should it replace labeled leukocyte scintigraphy of inpatients? *AJR Am J Roentgenol* 2019; **213**: 1358–65. doi: https://doi.org/10.2214/AJR.18.20475
17. Bhargava KK, Gupta RK, Nichols KJ, Palestro CJ. In vitro human leukocyte labeling with (64)Cu: an intraindividual comparison with (111)In-oxine and (18)F-FDG. *Nucl Med Biol* 2009; **36**: 545–9. doi: https://doi.org/10.1016/j.nucmedbio.2009.03.001
18. Man F, Khan AA, Carrascal-Miniño A, Blower PJ, T.M. de Rosales R. A kit formulation for the preparation of [89Zr] Zr(oxinate)4 for PET cell tracking: White blood cell labelling and comparison with [111In]In(oxinate)3. *Nucl Med Biol* 2020; **90-91**: 31–40. doi: https://doi.org/10.1016/j.nucmedbio.2020.09.002